Materials and Methods

Animals

The experiments were performed on 10 Tg and 10 littermate WT New Zealand White rabbits. Our techniques for generating Tg rabbits have been described in detail.[13] This study was conducted in accordance with the ARVO Statement for the Use of Animals in Ophthalmic and Vision Research. All protocols were approved by the Animal Research Review Board of Nagoya University Graduate School of Medicine (no. 23005).

ERG Recordings

Each animal was anesthetized with an intramuscular injection of 25 mg/kg ketamine and 2 mg/kg xylazine. ERGs were recorded with a bipolar contact lens electrode (GoldLens; Doran Instruments, Littleton, MA). Animals were placed in a Ganzfeld bowl and stimulated with stroboscopic stimuli (model SG-2002; LKC Technologies, Gaithersburg, MD). The full-strength stimulus was attenuated with neutral density filters in 0.5-log unit steps. Photopic ERGs were recorded after 10 minutes of light adaptation, and the stimulus strength ranged from 0.2 to 2.2 log cd-s/m^2 (photopic unit), and they were presented on a rod-suppressing white background of 3.3 log scot td. Signals were amplified, band pass-filtered between 0.3 to 1000 Hz, and averaged using a computer-assisted signal analysis system (MEB-9100; Neuropack, Nihon Kohden, Tokyo, Japan).

Drug Injections

Drugs and techniques for the intravitreal injections have been described in detail.[15,16,18] The drugs were dissolved in sterile PBS, and the pH was titrated to 7.4 with hydrochloric acid or sodium hydrate. The drugs were injected into the vitreous with a 30-gauge needle inserted through the pars plana approximately 1 mm posterior to the limbus.

Two types of glutamate analogs—(±)-2 amino-4-phosphonobutyric acid (APB; Sigma-Aldrich Japan, Tokyo, Japan) and 6-cyano-7-nitroquinoxaline-2,3(1H,4H)-dione (CNQX, Sigma-Aldrich Japan)—were used. APB is an agonist of the type 6 metabotropic glutamate receptor, and it blocks signal transmission between the photoreceptors and depolarizing or ON-bipolar cells.[19] CNQX is an antagonist of the α-amino-3-hydroxy-5-methyl-4-isoxazolepropionic acid/kainic acid (AMPA/KA) class of ionotropic glutamate receptors and is known to block the light responses of the hyperpolarizing or OFF-bipolar cells, horizontal cells, and all third-order retinal neurons.[20] Thus, the combination of APB and CNQX is expected to isolate the photoreceptor responses. We could not use PDA,[21] another type of antagonist of the AMPA/KA class of ionotropic glutamate receptors, because PDA was not commercially available. Intravitreal concentrations were 2 to 4 mM for APB and 0.2 to 0.4 mM for CNQX, assuming that the vitreous volume of the NZW rabbit is 1.5 mL.[22] The drugs were dissolved in 0.05 mL saline.

Recordings were begun approximately 60 to 90 minutes after the drug injections, and studies were completed within 3 hours. Although the drug effects were reversible, we only used the rabbits that had not been used for any previous experiments.

Measurement of a-Waves

To determine the photoreceptor and post-photoreceptoral contributions to the a-wave of the photopic ERGs quantitatively, we measured the amplitude of the a-wave before and after drug administration. Before drug administration, the a-wave amplitude was measured from the baseline to the first negative trough; after it, the a-wave amplitude was measured from the baseline to the potential at the time of the a-wave peak before the drugs (Fig. 1A). Then the percentage cone photoreceptor contribution was calculated by the expression (a-wave amplitude after APB and CNQX)/(a-wave amplitude before drugs) × 100. This method has been used to determine the degree of cone photoreceptor contribution to the a-wave.[3]

Statistical Analysis

Because the data were normally distributed, unpaired Student's *t*-tests were used to determine whether the amplitude of the a-wave of WT rabbits was significantly different from that of Tg rabbits. Differences were considered to be significant when $P < 0.05$.

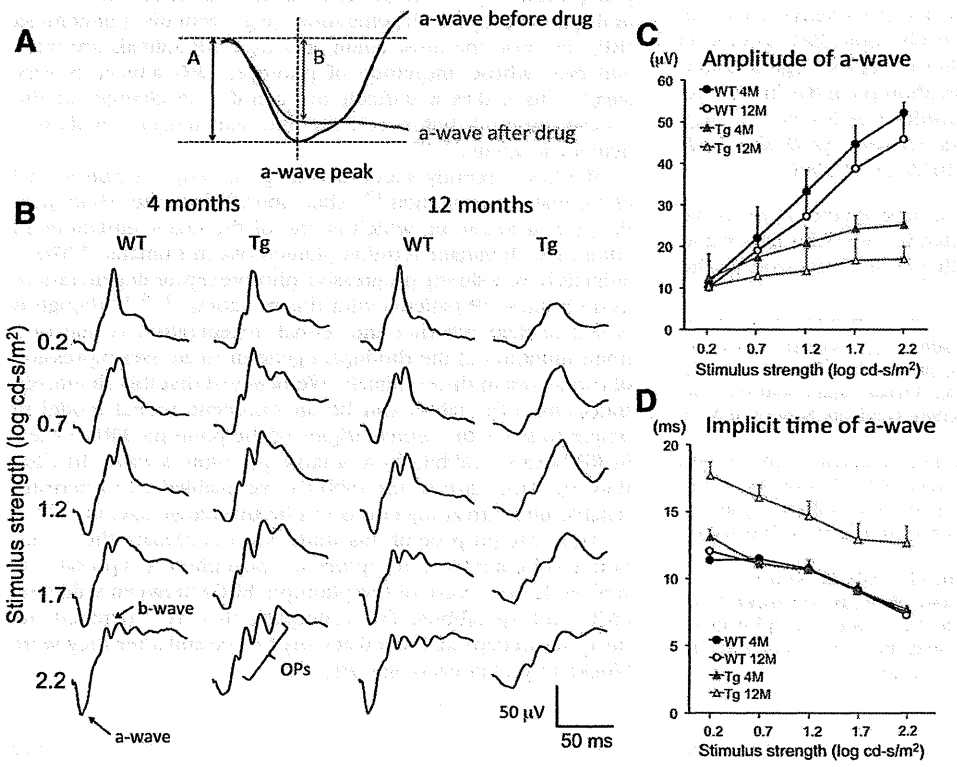

FIGURE 1. Photopic ERGs of WT and rhodopsin P347L Tg rabbits. (**A**) Method of measuring a-wave amplitude. The a-wave amplitude before drug administration was measured from the baseline to the first negative trough. (**B**) The a-wave amplitude after drug administration was measured from the baseline to the negative value at the time of the a-wave peak before drug administration. Representative photopic ERGs recorded from WT and Tg rabbits at 4 and 12 months of age. ERG waveforms to five different stimulus strengths of 0.2 to 2.2 log cd-s/m^2 are shown. (**C**) Plots of the a-wave amplitude to five different stimulus strengths. Results of WT and Tg rabbits at 4 and 12 months of age are shown. Bars indicate the SE of the means of five animals. (**D**) Plots of the a-wave implicit times to five different stimulus strengths. Results of WT and Tg rabbits at 4 and 12 months of age are shown. Bars indicate the SE of the means of five animals.

RESULTS

Photopic ERGs of WT and Tg Rabbits

Representative photopic ERGs recorded from WT and Tg rabbits at 4 and 12 months of age are shown in Figure 1B. The ERG waveforms elicited by five different stimulus strengths from 0.2 to 2.2 log cd-s/m^2 are shown. We found that all the ERG components of Tg rabbits decreased progressively with increasing age; the a-wave was more affected than the b-wave. These general ERG findings agree with the results reported in our earlier publications.[13,15]

The amplitudes of the a-waves of the photopic ERGs of Tg rabbits were significantly smaller than those of WT rabbits at 4 months of age and even smaller at 12 months of age (Figs. 1B, 1C). The implicit times of the photopic ERG a-wave were not significantly different between the Tg and WT rabbits when they were 4 months of age, but the Tg rabbits had severely delayed implicit times when they were 12 months of age (Fig. 1D).

Effect of APB or CNQX Alone on Photopic ERG a-Wave

To confirm that the a-waves of the photopic ERG in rabbits originated from the same neurons as macaque monkeys, we examined the effect of APB or CNQX alone on the a-wave of the photopic ERGs in WT and Tg rabbits when they were 4 months of age (Fig. 2). We found that intravitreal injection of APB did not alter the leading edge of the photopic a-wave, and the maximal a-wave amplitudes were nearly the same before and after the APB injection for both WT and Tg rabbits (Fig. 2, upper trace). In contrast, an intravitreal injection of CNQX significantly changed the leading edge of the a-wave, and the maximal a-wave amplitude was significantly reduced in both types of rabbits (Fig. 2, lower trace). These results were comparable to the results in primates[3–6] and support the belief that the photopic ERG a-wave receives significant contributions from post-photoreceptoral neurons, including OFF-bipolar cells and horizontal cells in both WT and Tg rabbits.

Amplitude Changes of Photopic ERG a-Wave after Pharmacologic Drug Administration

We next examined the contribution of the cone photoreceptors to the photopic ERG a-wave at the time of the a-wave peak. The black lines in Figure 3 show the photopic ERG a-waves before drugs, and the color lines (blue, WT; red, Tg) show the ERG waveforms after intravitreal injection of a solution of combined APB and CNQX (i.e., the cone photoreceptor response). The vertical dotted lines show the timing of the a-wave peaks before drug administration. As reported in primates,[3–6] the a-wave amplitude is greatly reduced after blocking all post-photoreceptoral neurons by glutamate analogs.

Mean amplitudes of the a-wave before and after drug administration at the time of the a-wave peak (Fig. 1A), are plotted in Figure 4. The a-wave amplitude decreased after injection of both APB and CNQX for all stimulus strengths in both WT and Tg rabbits.

Relative Contributions of Cone Photoreceptors to Photopic a-Wave

We next compared the relative contributions of the cone photoreceptors with the photopic ERG a-wave for the two types of rabbits. For this, we calculated the percentage contribution of the cone photoreceptors; that is, we divided the a-wave amplitude after APB+CNQX by the a-wave amplitude before drug administration (Fig. 5). We found that the percentage contribution of the cone photoreceptors became greater with increasing stimulus strengths in both WT and Tg rabbits, which is consistent with the findings in normal macaque monkeys.[3] The percentage contribution of the cone photoreceptors ranged from 32% to 51% in Tg rabbits, which was significantly smaller than that in WT rabbits at 54% to 75%, at 4 months of age ($P < 0.01$; Fig. 5, left).

We also calculated these values when the animals were 12 months of age. The percentage contribution of the cone photoreceptors ranged from 11% to 48% in Tg rabbits, which was also significantly smaller than that in WT rabbits at 41% to 70% ($P < 0.05$; Fig. 5, right). The percentage contribution of cone

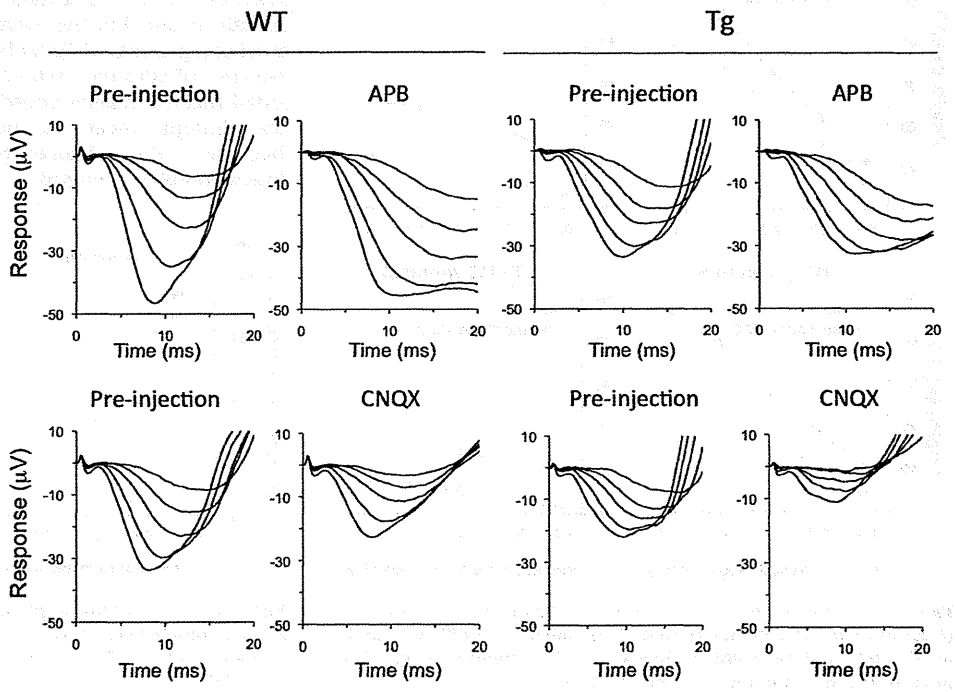

FIGURE 2. Representative waveforms of photopic ERG a-wave before and after APB or CNQX alone in WT and Tg rabbits of 4 months of age. ERG waveforms to five different stimulus strengths of 0.2 to 2.2 log cd-s/m^2 are superimposed.

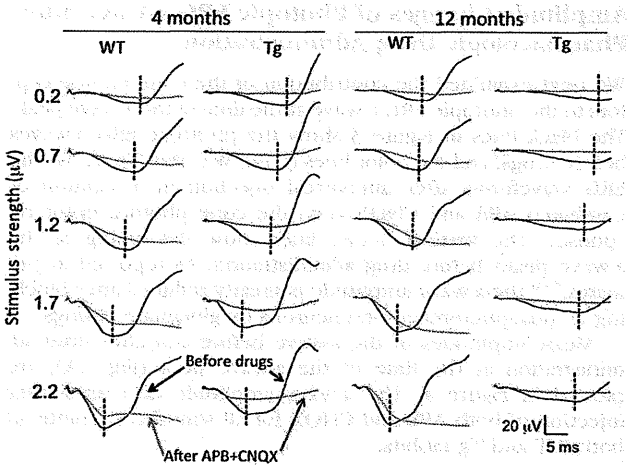

FIGURE 3. Representative waveforms of photopic ERG a-wave before (*black*) and after (*blue* and *red*) intravitreal injection of combination of APB and CNQX in WT and Tg rabbits at 4 and 12 months of age. *Vertical dotted lines*: timing of the a-wave peaks before drug administration.

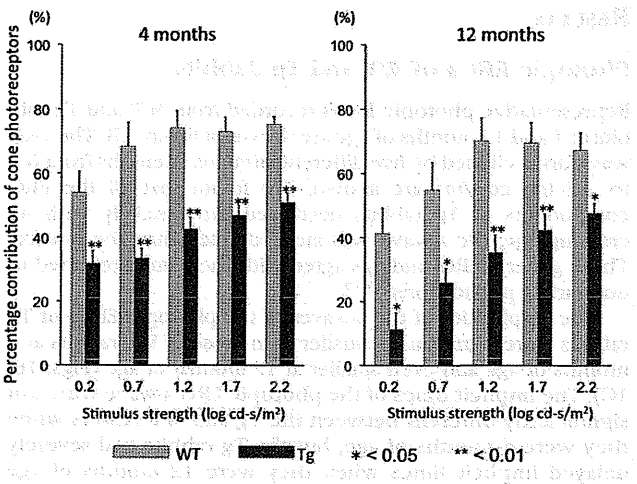

FIGURE 5. Plots of the percentage contribution of cone photoreceptors to the photopic ERG a-wave in WT (*blue*) and Tg (*red*) rabbits at 4 and 12 months of age. Bars indicate the SE of the means of five animals. $^{*}P < 0.05$; $^{**}P < 0.01$.

photoreceptors to the photopic a-wave in 12-month-old Tg rabbits was <50% for all stimulus strengths.

Comparison of Postreceptoral Components

The smaller contributions of cone photoreceptors to the photopic a-waves in Tg rabbits can be explained simply by a decrease in cone photoreceptor responses caused by the photoreceptor degenerations, which can be clearly seen in Figure 4. However, it can also be caused by an increase in neural activities of the post-photoreceptoral neurons. To investigate whether the latter explanation was the cause, we calculated the amplitudes of post-photoreceptoral components at the time of the a-wave peak by subtracting the post-APB+CNQX waveform from the predrug waveform. Results are plotted in Figure 6.

Although the maximal amplitudes of the post-photoreceptoral components were not significantly different in WT and Tg rabbits, the intensity amplitude function for the two types of rabbits were different when they were 4 months of age (Fig. 6, left). The amplitude of the post-photoreceptoral component was nearly saturated at lower stimulus strengths of 0.7 to 1.2 log cd-s/m^2 in Tg rabbits. In contrast, this value increased gradually and reached maximum amplitude at the highest stimulus strength of 2.2 log cd-s/m^2 in WT rabbits. The amplitudes of the post-photoreceptoral components in Tg rabbits were significantly larger than those in WT rabbits at lower stimulus strengths of 0.2 and 0.7 log cd-s/m^2 ($P < 0.05$).

A similar tendency of the stimulus strength-amplitude functions of WT and Tg rabbits was also seen when they were 12 months of age, but the overall amplitudes of post-photoreceptoral components of Tg rabbits were greatly reduced, probably because of advanced retinal degeneration. These results indicated that the smaller contribution of cone photoreceptors to the photopic a-wave in young Tg rabbits occurred partially because of the enhanced post-photoreceptoral responses at lower stimulus strengths.

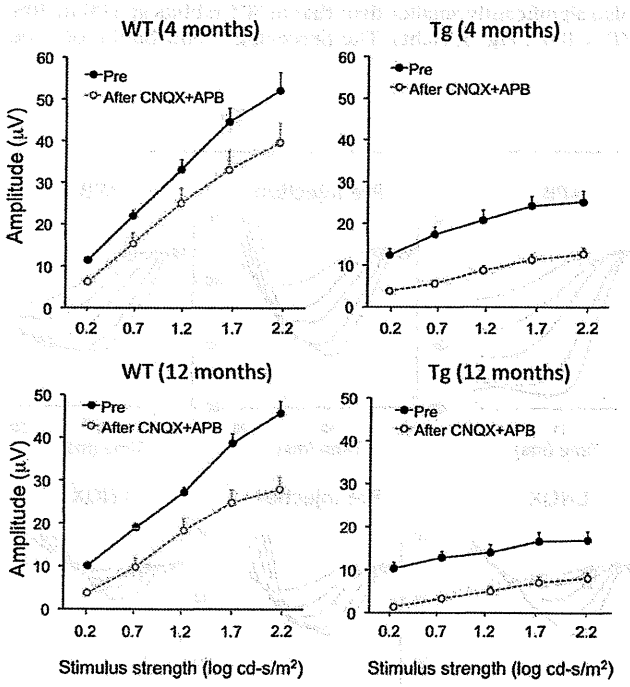

FIGURE 4. Plots of the a-wave amplitude before (*black*) and after (*blue* and *red*) intravitreal injection of combination of APB and CNQX in WT (*left*) and Tg (*right*) rabbits at 4 and 12 months of age. Bars indicate the SE of the means of five animals.

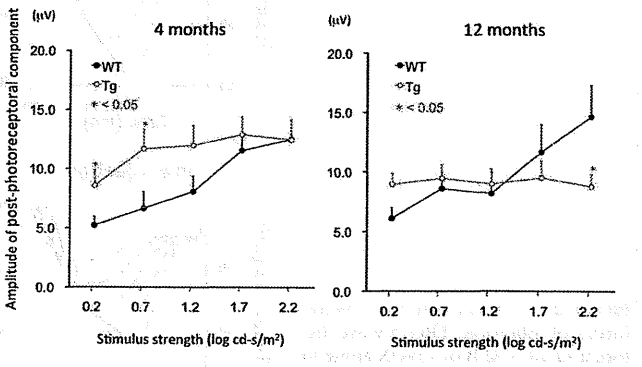

FIGURE 6. Plots of the amplitude of post-photoreceptoral component in the photopic ERG a-wave in WT (*black*) and Tg (*red*) rabbits at 4 and 12 months of age. Bars indicate the SE of the means of five animals. $^{*}P < 0.05$.

Discussion

It is unknown whether the contributions of photoreceptors and post-photoreceptoral neurons are altered in retinas with progressive photoreceptor degeneration. Our present results clearly demonstrated that the percentage contribution of the cone photoreceptors to the photopic a-wave was significantly lower in rhodopsin P347L Tg rabbits than in WT rabbits over a 2 log unit range of stimulus strengths at both 4 and 12 months of age. We found that especially in the retina of 12-month-old Tg rabbits, the percentage contribution of cone photoreceptor to the photopic ERG a-wave was less than half, irrespective of the stimulus strength (Fig. 5, right).

Our results showed that the effects of stimulus strength on the cone photoreceptors and post-photoreceptoral contributions to the photopic a-wave of normal retinas were similar to those in primates reported by Bush and Sieving.[3] They measured the degree of cone photoreceptor and post-photoreceptoral contribution to the photopic a-wave at the time of the a-wave peak in normal macaque monkeys before and after APB and PDA. They did not report the exact percentage values, but they showed[3] that it was relatively low at 55% at the lowest stimulus strengths and that it gradually increased to a maximum of 92% at the highest stimulus strength. They interpreted these findings that the post-photoreceptoral contribution to the photopic a-wave was primarily responsible for the initial 1 to 1.5 log units of strength, whereas cone photoreceptor contribution progressively dominated the photopic a-wave at higher stimulus strengths. We also observed a similar pattern in our WT rabbits (Fig. 5), but the percentage contribution of cone photoreceptor at the highest stimulus strength was higher in macaque (92%) than in our WT rabbits (75%). This difference might have been due to the difference in the type of stimulus (200-ms long-flash stimuli in their study vs. xenon brief-flash stimuli in our study) or difference in species.

We found that the percentage contribution of cone photoreceptors to the photopic a-wave in Tg rabbits was significantly lower than in WT rabbits (Fig. 5). These results are reasonable because the cone photoreceptor is gradually attenuated whereas the middle and inner retinas are still well preserved in Tg rabbits.[13,15] Additional analyses demonstrated that the smaller percentage contribution of cone photoreceptors in young Tg rabbits can be explained, in part, by the enhancement of the amplitudes of the post-photoreceptoral component, especially at lower stimulus strengths (Fig. 6, left). Such enhanced amplitudes of the post-photoreceptoral component in Tg rabbits were no longer present at 12 months in Tg rabbits, probably because of advanced retinal degeneration.

We do not know the exact mechanism for the enhanced amplitudes of the post-photoreceptoral components elicited by weaker stimulus intensities in young Tg rabbits. This enhanced post-photoreceptoral response may be due to secondary functional changes in the OFF-bipolar/horizontal cells or their synapses after progressive photoreceptor degenerations.

Using computational molecular phenotyping, we have recently shown that during the course of rod photoreceptor degeneration, rod ON-bipolar cells switch their phenotype by expressing ionotropic glutamate receptors (iGluRs).[17] We also found that the rod bipolar cells effectively lose rod contacts and make ectopic cone contacts and express iGluRs.[17] This secondary retinal remodeling may contribute to the enhanced post-photoreceptoral responses in our Tg rabbits. Similarly, detailed ERG studies in rhodopsin P347L Tg pigs and rabbits have demonstrated that the electrical activities of the cone ON-pathway were also enhanced at a relatively early stage of retinal degeneration.[18,23] In addition, an increase in the ERG responses from the inner retina (e.g., scotopic threshold response) was also reported in the retina of the aged Royal College of Surgeons rat, a rodent model of retinal degeneration.[24,25]

Taken together, inherited retinal diseases associated with progressive photoreceptor degeneration may lead to different types of functional changes in the post-photoreceptoral retinal circuits, including the ON- and OFF pathways, during a relatively early stage of retinal degeneration.

We believe our results have important clinical implications. The a-wave of the photopic ERG is believed to be shaped primarily by electrical activities of cone photoreceptors in patients. However, the results of this study suggest that the cone photoreceptor function may be overestimated when the amplitude of the cone ERG a-wave is used as an indicator of residual cone photoreceptor functions in patients with progressive photoreceptor degeneration such as RP. Thus, when the standard stimulus strength (3.0 cd-s/m^2 = 0.48 log cd-s/m^2) recommended by the International Society of Clinical Electrophysiology of Vision[1] was used, contributions of the cone photoreceptors to the photopic a-wave was only 34% at the time of the a-wave peak, and the other 66% originated from post-photoreceptoral neurons (Fig. 5, left). Our results suggest that the lower contribution of the cones to the a-waves of the photopic ERGs must be considered in patients with RP.

There are limitations to this study. One was that we assessed the contribution of photoreceptors and post-photoreceptoral components only at the time of the a-wave peak before the drugs. However, the peak time of the a-wave depends on not only the stimulus strength but also on the presence of retinal degeneration (Fig. 1D). In addition, the a-wave can be truncated by the b-wave. To overcome this, we measured the a-wave amplitude at specific times before the b-wave intrusion (10.5 ms for 0.2 log cd-s/m^2, 9.5 ms for 0.7 log cd-s/m^2, 8.5 ms for 1.2 log cd-s/m^2, 7.5 ms for 1.7 log cd-s/m^2, and 6.5 ms for 2.2 log cd-s/m^2), and calculated the percentage cone photoreceptor contribution when the animals were 4 months of age. We found that the cone photoreceptor contribution still tended to be smaller in Tg rabbits than in WT rabbits, and the differences were significant at the two lower stimulus strengths ($P < 0.01$, Supplementary Fig. S1A, http://www.iovs.org/lookup/suppl/doi:10.1167/iovs.11-9006/-/DCSupplemental). We also measured the a-wave amplitude at a single constant time of 7 ms and calculated the percentage cone photoreceptor contribution. Again, the cone photoreceptor contribution tended to be smaller in Tg rabbits than in WT rabbits, but the difference was significant only at the highest stimulus strength (Supplementary Fig. S1B, http://www.iovs.org/lookup/suppl/doi:10.1167/iovs.11-9006/-/DCSupplemental).

In summary, our results indicate that the relative contribution of cone photoreceptors to the photopic ERG a-wave is smaller in retinas with inherited photoreceptor degeneration. These results suggest that care must be taken in interpreting the a-wave amplitudes of photopic ERGs in patients with progressive photoreceptor degeneration.

Acknowledgments

The authors thank Duco I. Hamasaki for editing the manuscript and Michael Bach for helpful discussions.

References

1. Marmor MF, Fulton AB, Holder GE, et al. ISCEV Standard for full-field clinical electroretinography (2008 update). *Doc Ophthalmol.* 2009;118:69–77.
2. Frishman LJ. Origins of the electroretinogram. In: Heckenlively JR, Arden GB, eds. *Principles and Practice of Clinical Electrophysiology of Vision*. 2nd ed. London: MIT Press; 2006:139–183.
3. Bush RA, Sieving PA. A proximal retinal component in the primate photopic ERG a-wave. *Invest Ophthalmol Vis Sci.* 1994;35:635–645.

4. Sieving PA, Murayama K, Naarendorp F. Push-pull model of the primate photopic electroretinogram: a role for hyperpolarizing neurons in shaping the b-wave. *Vis Neurosci.* 1994;11:519–532.
5. Jamison JA, Bush RA, Lei B, Sieving PA. Characterization of the rod photoresponse isolated from the dark-adapted primate ERG. *Vis Neurosci.* 2001,18:445–455.
6. Robson JG, Saszik SM, Ahmed J, Frishman LJ. Rod and cone contributions to the a-wave of the electroretinogram of the macaque. *J Physiol.* 2003;547:509–530.
7. Friedburg C, Allen CP, Mason PJ, Lamb TD. Contribution of cone photoreceptors and post-receptoral mechanisms to the human photopic electroretinogram. *J Physiol.* 2004;556:819–834.
8. Sharma S, Ball SL, Peachey NS. Pharmacological studies of the mouse cone electroretinogram. *Vis Neurosci.* 2005;22:631–636.
9. Bui BV, Fortune B. Origin of electroretinogram amplitude growth during light adaptation in pigmented rats. *Vis Neurosci.* 2006;23:155–67.
10. Koyasu T, Kondo M, Miyata K, et al. Photopic electroretinograms of mGluR6-deficient mice. *Curr Eye Res.* 2008;33:91–99.
11. Miura G, Wang MH, Ivers KM, Frishman LJ. Retinal pathway origins of the pattern ERG of the mouse. *Exp Eye Res.* 2009;89:49–62.
12. Shirato S, Maeda H, Miura G, Frishman LJ. Postreceptoral contributions to the light-adapted ERG of mice lacking b-waves. *Exp Eye Res.* 2008;86:914–928.
13. Kondo M, Sakai T, Komeima K, et al. Generation of a transgenic rabbit model of retinal degeneration. *Invest Ophthalmol Vis Sci.* 2009;50:1371–1377.
14. Dryja TP, Hahn LB, Cowley GS, et al. Mutation spectrum of the rhodopsin gene among patients with autosomal dominant retinitis pigmentosa. *Proc Natl Acad Sci U S A.* 1991;88:9370–9374.
15. Sakai T, Kondo M, Ueno S, et al. Supernormal ERG oscillatory potentials in transgenic rabbit with rhodopsin P347L mutation and retinal degeneration. *Invest Ophthalmol Vis Sci.* 2009;50:4402–449.
16. Yokoyama D, Machida S, Kondo M, et al. Pharmacological dissection of multifocal electroretinograms of rabbits with Pro347Leu rhodopsin mutation. *Jpn J Ophthalmol.* 2010;54:458–466.
17. Jones BW, Kondo M, Terasaki H, et al. Retinal remodeling in the Tg P347L rabbit, a large-eye model of retinal degeneration. *J Comp Neurol.* 2011;519:2713–2733.
18. Nishimura T, Machida S, Kondo M, et al. Enhancement of ON-bipolar cell responses of cone electroretinograms in rabbits with Pro347Leu rhodopsin mutation. *Invest Ophthalmol Vis Sci.* 2011;52:7610–7617.
19. Slaughter MM, Miller RF. 2-Amino-4-phosphonobutyric acid: a new pharmacological tool for retina research. *Science.* 1981;211:182–185.
20. Honoré T, Davies SN, Drejer J, et al. Quinoxalinediones: potent competitive non-NMDA glutamate receptor antagonists. *Science.* 1988;241:701–703.
21. Slaughter MM, Miller RF. An excitatory amino acid antagonist blocks cone input to sign-conserving second-order retinal neurons. *Science.* 1983;219:1230–1232.
22. Leeds JM, Henry SP, Truong L, et al. Pharmacokinetics of a potential human cytomegalovirus therapeutic, a phosphorothioate oligonucleotide, after intravitreal injection in the rabbit. *Drug Metab Dispos.* 1997;25:921–926.
23. Banin E, Cideciyan AV, Alemán TS, et al. Retinal rod photoreceptor-specific gene mutation perturbs cone pathway development. *Neuron.* 1999;23:549–557.
24. Bush RA, Hawks KW, Sieving PA. Preservation of inner retinal responses in the aged Royal College of Surgeons rat: evidence against glutamate excitotoxicity in photoreceptor degeneration. *Invest Ophthalmol Vis Sci.* 1995;36:2054–2062.
25. Machida S, Raz-Prag D, Fariss RN, et al. Photopic ERG negative response from amacrine cell signaling in RCS rat retinal degeneration. *Invest Ophthalmol Vis Sci.* 2008;49:442–452.

OPEN ACCESS Freely available online

PLoS one

Identification of Autoantibodies against TRPM1 in Patients with Paraneoplastic Retinopathy Associated with ON Bipolar Cell Dysfunction

Mineo Kondo[1*☯], Rikako Sanuki[2,3☯], Shinji Ueno[1], Yuji Nishizawa[4], Naozumi Hashimoto[5], Hiroshi Ohguro[6], Shuichi Yamamoto[7], Shigeki Machida[8], Hiroko Terasaki[1], Grazyna Adamus[9], Takahisa Furukawa[2,3*]

1 Department of Ophthalmology, Nagoya University Graduate School of Medicine, Nagoya, Aichi, Japan, **2** Department of Developmental Biology, Osaka Bioscience Institute, Suita, Osaka, Japan, **3** JST, CREST, Suita, Osaka, Japan, **4** Department of Biomedical Sciences, Chubu University, Kasugai, Aichi, Japan, **5** Department of Respiratory Medicine, Nagoya University Graduate School of Medicine, Nagoya, Aichi, Japan, **6** Department of Ophthalmology, Sapporo Medical University School of Medicine, Sapporo, Hokkaido, Japan, **7** Department of Ophthalmology and Visual Science, Chiba University Graduate School of Medicine, Chiba, Chiba, Japan, **8** Department of Ophthalmology, Iwate Medical University School of Medicine, Morioka, Iwate, Japan, **9** Department of Ophthalmology, Oregon Health and Science University, Portland, Oregon, United States of America

Abstract

Background: Paraneoplastic retinopathy (PR), including cancer-associated retinopathy (CAR) and melanoma-associated retinopathy (MAR), is a progressive retinal disease caused by antibodies generated against neoplasms not associated with the eye. While several autoantibodies against retinal antigens have been identified, there has been no known autoantibody reacting specifically against bipolar cell antigens in the sera of patients with PR. We previously reported that the transient receptor potential cation channel, subfamily M, member 1 (TRPM1) is specifically expressed in retinal ON bipolar cells and functions as a component of ON bipolar cell transduction channels. In addition, this and other groups have reported that human TRPM1 mutations are associated with the complete form of congenital stationary night blindness. The purpose of the current study is to investigate whether there are autoantibodies against TRPM1 in the sera of PR patients exhibiting ON bipolar cell dysfunction.

Methodology/Principal Findings: We performed Western blot analysis to identify an autoantibody against TRPM1 in the serum of a patient with lung CAR. The electroretinograms of this patient showed a severely reduced ON response with normal OFF response, indicating that the defect is in the signal transmission between photoreceptors and ON bipolar cells. We also investigated the sera of 26 patients with MAR for autoantibodies against TRPM1 because MAR patients are known to exhibit retinal ON bipolar cell dysfunction. Two of the patients were found to have autoantibodies against TRPM1 in their sera.

Conclusion/Significance: Our study reveals TRPM1 to be one of the autoantigens targeted by autoantibodies in at least some patients with CAR or MAR associated with retinal ON bipolar cell dysfunction.

Citation: Kondo M, Sanuki R, Ueno S, Nishizawa Y, Hashimoto N, et al. (2011) Identification of Autoantibodies against TRPM1 in Patients with Paraneoplastic Retinopathy Associated with ON Bipolar Cell Dysfunction. PLoS ONE 6(5): e19911. doi:10.1371/journal.pone.0019911

Editor: Steven Barnes, Dalhousie University, Canada

Received February 10, 2011; **Accepted** April 6, 2011; **Published** May 17, 2011

Funding: This work was supported by CREST from the Japan Science and Technology Agency (http://www.jst.go.jp/), and a Grant-in-Aid for Scientific Research (B)(C) (#20390448, #20390087, #20592075, #20791678) from the Ministry of Education, Culture, Sports, Science and Technology (http://www.jsps.go.jp/), the Takeda Science Foundation (http://www.takeda-sci.or.jp/), The Uehara Memorial Foundation (http://www.ueharazaidan.com/), the Naito Foundation (http://www.naito-f.or.jp/), the Novartis Foundation (#20-10, http://novartisfound.or.jp/), Mochida Memorial Foundation for Medical and Pharmaceutical Research (http://www.mochida.co.jp/zaidan/), the Senri Life Science Foundation (#S-2144, http://www.senri-life.or.jp/), the Kato Memorial Bioscience Foundation (http://www.katokinen.or.jp/) and the Japan National Society for the Prevention of Blindness (http://www.nichigan.or.jp/link/situmei.jsp). A grant from the National Institute of Health (E13053), was awarded to GA. The funders had no role in study design, data collection and analysis, decision to publish, or preparation of the manuscript.

Competing Interests: The authors have declared that no competing interests exist.

* E-mail: furukawa@obi.or.jp (TF); kondomi@med.nagoya-u.ac.jp (MK)

☯ These authors contributed equally to this work.

Introduction

Paraneoplastic retinopathy (PR) is a progressive retinal disorder caused by an autoimmune mechanism and is associated with the presence of anti-retinal antibodies in the serum generated against neoplasms not associated with the eye [1–4]. The retinopathy can develop either before or after the diagnosis of a neoplasm. Patients with PR can have night blindness, photopsia, ring scotoma, attenuated retinal arteriole, and abnormal electroretinograms (ERGs). The diagnosis of PR is usually made by the identification of neoplasms and anti-retinal autoantibodies in the sera.

PR includes two subgroups: cancer-associated retinopathy (CAR) [5,6] and melanoma-associated retinopathy (MAR) [7–10]. Although CAR and MAR share similar clinical symptoms, the ERG findings

are very different. Both a- and b-waves are severely attenuated in CAR, indicating extensive photoreceptor dysfunction, whereas only the b-wave is severely reduced while the a-wave is normal in MAR, suggesting bipolar cell dysfunction [8,9]. However, it was recently reported that cancers other than melanoma can cause bipolar cell dysfunction [11,12]. Several autoantibodies against retinal antigens have been identified, but a specific antigen associated with bipolar cells has not been identified in patients with CAR and MAR [1–10].

In the current study, we identified autoantibodies against the transient receptor potential cation channel, subfamily M, member 1 (TRPM1) [13–15] in the serum of one patient with lung cancer. The ERG findings in this patient indicated a selective ON-bipolar cell dysfunction. We also investigated the sera of 26 MAR patients and found that two contained autoantibodies against TRPM1. Our results suggest that TRPM1 is one of the retinal autoantigens in at least some patients with CAR or MAR and may cause retinal ON bipolar cell dysfunction.

Results

Case report of CAR associated with ON bipolar cell dysfunction

A 69-year-old man visited the Nagoya University Hospital with complaints of blurred vision, photopsia and night blindness in both eyes of three months duration. At this point he was not diagnosed as suffering from any eye disease or systemic disease, including a malignant tumor, and his family history revealed no other members suffering from any eye diseases. On initial examination, his best-corrected visual acuity was 0.9 in the right eye and 0.6 in the left eye. Humphrey static perimetry revealed a severe decrease in sensitivity within the central 30 degrees of the visual field in both eyes (Fig. 1A). Dark-adaptometry of this patient showed a loss of the rod branch. The cone threshold was within normal range. Ophthalmoscopy showed a nearly normal fundus appearance except for slight hypopigmentation at the macula of the left eye, which may be due to age-related changes in the retinal pigment epithelium (Fig. 1B), but fluorescein angiography demonstrated periphlebitis of the retinal vessels (arrows, Fig. 1C). Spectral-domain optical coherence tomography (SD-OCT) showed that the morphology of the retina was normal in both eyes (Fig. 1D).

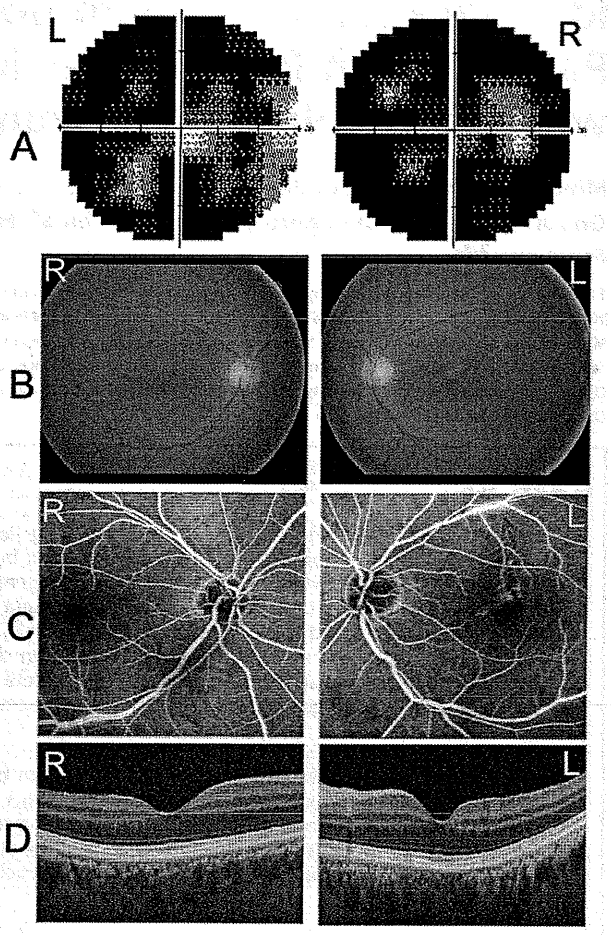

Figure 1. Ophthalmological findings from a patient with paraneoplastic retinopathy (PR) associated with lung cancer. (A) Threshold of static visual field (Humphrey, 30-2 program) plotted on a gray scale showing severely decreased sensitivities within the central 30 degrees of the visual field. (B) Fundus photographs of the patient showing a nearly normal fundus. (C) Fluorescein angiograms showing periphlebitis of the retinal vessels (arrows). (D) Spectral-domain optical coherence tomographic (SD-OCT) image of a 9 mm horizontal scan of the retina of our patient. The retinal structure in each retinal layer is normal.
doi:10.1371/journal.pone.0019911.g001

Electrophysiological examinations

Recordings of the full-field ERGs from this patient showed that the rod responses were undetectable (Fig. 2). The rod- and cone-mixed maximal response was a negative-type with an a-wave of normal amplitude and a b-wave that was smaller than the a-wave. The a-wave of the cone response had a wide trough, and the b-wave was reduced by 40%. The amplitude of the 30-Hz flicker ERG was reduced by 50%. The photopic long-flash ERG showed severely reduced ON response and normal OFF response. These ERG findings indicated that there was a defect in the signal transmission from photoreceptors to ON bipolar cells both in both rod and cone pathways.

Based on these ophthalmological and electrophysiological tests, we suspected that this patient might have PR and referred him to an internist. The general physical examination including positron emission tomography and computed tomography revealed two abnormal masses in the right lung. Biopsy of these masses confirmed that the masses were small cell carcinomas of the lung.

Detection of autoantibodies against TRPM1 in the serum of the CAR patient

Based on our ERG examination results, we hypothesized that the serum of this CAR patient may contain autoantibodies against TRPM1. To test this hypothesis, we examined whether or not this CAR patient's serum could recognize human TRPM1 protein by Western blot analysis. We transfected an expression plasmid containing human TRPM1 cDNA with the C-terminal 3xFlag-tag (TRPM1-3xFlag) into HEK293T cells, and carried out a Western blot analysis using whole cell extracts harvested after 48 hrs cell growth. We first confirmed that TRPM1-3xFlag was expressed by cell using Western blot analysis and an anti-Flag antibody. We detected the ~200 kDa TRPM1-3xFlag band in the cell lysates (Fig. 3A).

Next, we performed Western blot analysis on the same lysates using the serum from our CAR patient and a healthy control person. We detected immunostaining of the same size protein, which was confirmed with the anti-Flag antibody, and with CAR serum. The control serum did not present a significant band (Fig. 3B, C). This result showed the presence of autoantibodies against TRPM1 in this CAR patient's serum.

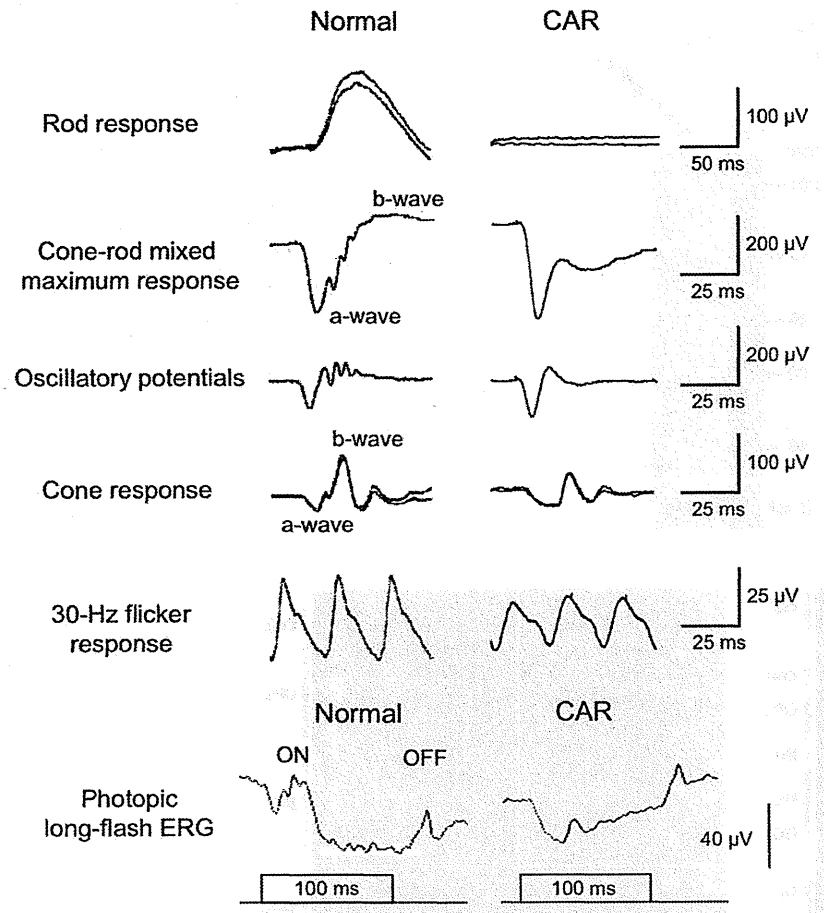

Figure 2. Full-field ERG recordings. The rod response was recorded with a blue light at an intensity of 5.2×10^{-3} cd-s/m^2 after 30 minutes of dark-adaptation. The cone-rod mixed maximum response was elicited by a white flash at an intensity of 44.2 cd-s/m^2. The oscillatory potentials were recorded with a white flash at an intensity of 44.2 cd-s/m^2 using a band-pass filter of 50–1000 Hz. The cone response and a 30 Hz flicker response were elicited by a white stimulus of 4 cd-s/m^2 and 0.9 cd-s/m^2, respectively, on a blue background of 30 cd/m^2. Photopic long-flash ERG responses were also elicited by long-duration flashes of 100 ms using a densely-packed array of white LEDs of 200 cd/m^2 on a white background of 30 cd/m^2.
doi:10.1371/journal.pone.0019911.g002

To examine whether the serum from the CAR patient recognized retinal bipolar cells, we carried out an immunohistochemical analysis on monkey and mouse retinas. We first performed immunohistochemistry on the retina of a 3-year-old rhesus monkey (*Macaca mulata*) and on the retina of a one-month-old C57/B6 mouse using the serum of the CAR patient, however, we did not obtain a significant staining signal above background (data not shown). We then concentrated the serum by IgG purification followed by filter spin column centrifugation and performed immunohistochemistry on the monkey retina using the concentrated serum (Fig. 3D–G). We observed a significant immunolabeling on the INL in the monkey retina (Fig. 3D, F) whereas the normal serum did not give a significant labeling (Fig. 3E, G). The antibodies immunolabeled both the bipolar side and amacrine side of the INL. Since most of the cells residing on the outer side of the INL are ON bipolar cells, at least some of the stained cells are ON bipolar cells. It should be noted some of the staining signals show a spotted pattern in the outer plexiform layer (Fig. 3F) as is observed in TRPM1 or mGluR6 immunostaining on the mouse retina [13], suggesting that the CAR patient serum recognizes the bipolar dendritic tips where some of the TRPM1 protein localizes.

Western blot analysis of the sera from MAR patients

Since the functional defect in the retina of MAR patients is known to be due to abnormal signal transmission between photoreceptors and ON bipolar cells [8,9], we then investigated whether or not autoantibodies to TRPM1 were also present in the sera of MAR patients. We obtained the sera of 26 MAR patients from two hospitals in Japan (Chiba University Hospital and Iwate Medical University Hospital) and Ocular Immunology Laboratory in the USA (Casey Eye Institute). We found that the sera from patients #8 and #23 exhibited a significant immunoreactive band against TRPM1-transfected cell lysates by Western blot analysis (Fig. 4A and B). The control serum showed no significant immune response against the TRPM1-transfected cell lysates (Fig. 3C). These results suggest that the sera from some MAR patients contain autoantibodies against TRPM1. Due to the limited volume of sera from the MAR patients, we could not try immunostaining on the monkey or the mouse retina using the serum from the patients #8 and #23.

MAR patient #8, was a 76-year-old man with a history of skin melanoma. He had ring scotomas and abnormal ERGs indicating that he had MAR. The other patient, MAR #23, was a 57-year-

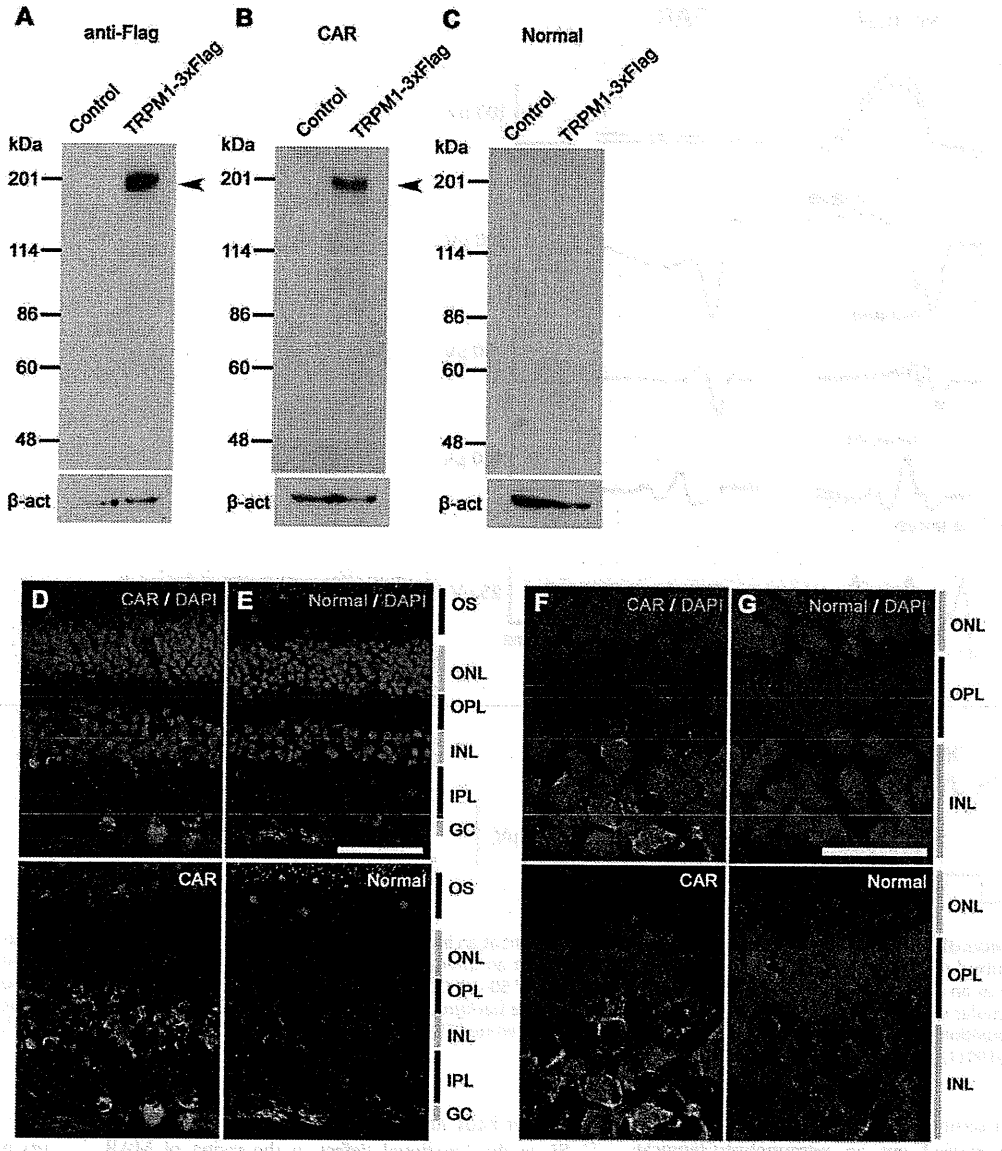

Figure 3. Immunostaining and Western blot analysis of human TRPM1 using serum from the CAR patient. (A–C) Immunoblots of the transfected cell lysates using an antibody against Flag tag (A), serum from CAR patient (B), and control serum (C). Arrowheads indicate the TRPM1-3xFlag protein bands. HEK293T cells were transfected with the pCAGGS or pCAGGS-human TRPM1-3xFlag plasmid, and cells were harvested after 48 hrs. β-actin (β-act) was used for a loading control. (D–G) Confocal images of a three-year-old rhesus monkey retina immunostained with the concentrated serum from the CAR patient (D, F) or the concentrated normal serum (E, G). Cell nuclei are visualized with DAPI. CAR patient serum presented signals on INL cells and the inner part of the OPL (D, F). Scale bar = 50 μm in (E) and 20 μm in (G).
doi:10.1371/journal.pone.0019911.g003

old man with poor night vision, abnormal scotopic ERGs and abnormal color vision. He had a history of skin melanoma and thyroid cancer. There was no other clinical information available on these two patients because these sera were obtained from other institutes several years before without detailed clinical information.

Discussion

PR, including MAR and CAR, presents visual disorders associated with systemic cancer. Antibodies against retinal cells and proteins have been detected in the sera of patients with PR suggesting an autoimmune basis for the etiology of the PR. The autoantibodies identified so far include rhodopsin, retinal transducin alpha and beta, recoverin, S-arrestin, α-enolase, carbonic anhydrase II, and heat shock protein-60 which reside abundantly in photoreceptors [1–10,16]. MAR and CAR can cause bipolar cell dysfunction [7–12]. The results of the ERG [8,9] and immunohistochemistry [7] studies suggested that the main target of MAR are retinal ON bipolar cells in both the rod and cone pathways. However, autoantibodies specifically reacting with a bipolar cell antigen had not been identified in the sera of patients with PR, including those with CAR and MAR. In the current study, we identified autoantibodies against TRPM1, a component of the ON bipolar cell transduction channel negatively regulated by Goα in the mGluR6 signaling pathway [13–15], in the

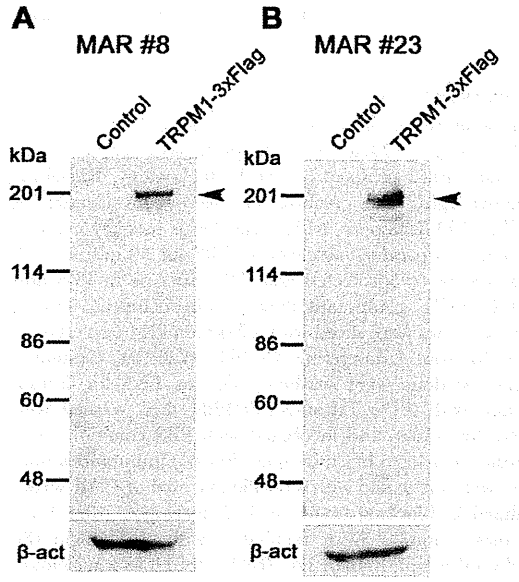

Figure 4. Western blot analysis of human TRPM1 using sera from the MAR patients. (A, B) Immunoblots of the transfected cell lysates using sera from MAR patient #8 (A) and MAR patient #23 (B). HEK293T cells were transfected with pCAGGS or pCAGGS-human TRPM1-3xFlag plasmid, and cells were harvested after 48 hrs. Arrowheads indicate the TRPM1-3xFlag protein bands. β-actin (β-act) was used for a loading control.
doi:10.1371/journal.pone.0019911.g004

sera of one CAR patient and two MAR patients. The CAR patient exhibited a dysfunction of ON bipolar cells, and to our knowledge, this is the first report on an autoantibody against a bipolar cell antigen in the serum of PR patients affecting the ON bipolar cell function.

Previously, we isolated a mouse *TRPM1-L* cDNA corresponding to the human long form of *TRPM1*, and found that the TRPM1-L protein is developmentally localized at the tips of the ON bipolar dendrites co-localizing with mGluR6, but not on OFF bipolar cells [13,14]. The *TRPM1* null mutant mouse completely loses the ON bipolar cell photoresponses to light, indicating that TRPM1 plays a critical role in the synaptic transmission from photoreceptors to ON-bipolar cells [13,15]. In addition, we demonstrated using a CHO cell reconstitution system that TRPM1-L is a nonselective cation channel which is negatively regulated by Goα downstream of the mGluR6 signaling cascade in ON bipolar cells [13]. Recently, four groups including ours independently reported that mutations of human *TRPM1* are associated with the complete-type of congenital stationary night blindness (cCSNB), an inherited human retinal disease [17–20]. cCSNB is a non-progressive retinal disease characterized by congenital night blindness with a moderate decrease in visual acuity and myopia [21-24]. Previous ERG studies have suggested that the defect in cCSNB patients lies in the signal transmission from photoreceptors to ON bipolar cells in both the rod and cone pathways [25–28]. We have identified five different mutations in our three cCSNB patients, and have shown that these mutations lead to either abnormal TRPM1 protein production or mislocalization of the TRPM1 protein in bipolar cell dendrites [17]. These results suggest that TRPM1 plays a critical role in mediating the photoresponses of ON bipolar cells in humans as well. Based on these findings, we hypothesize that the ectopic expression of TRPM1 in tumor cells of some CAR and MAR patients may result in aberrant production of autoantibodies to TRPM1 through B-lymphocytic responses [29–32]. These antibodies may react to the TRPM1 protein in retinal ON bipolar cells resulting in dysfunction of the TRPM1 transduction cation channel downstream of the mGluR6 signaling cascade. However, we could not confirm whether TRPM1 is expressed in the tumor cells of the three PR patients examined in this study [29] because tumor samples were not available.

Another question regarding the disease mechanism underlying PR is whether the binding of TRPM1 autoantibody to bipolar cells results in the cell death or dysfunction of bipolar cells. As far as we examined the retinal structure of the CAR patient using a spectral domain optical coherence tomography (SD-OCT) retinal imaging device, the structure of the retinal bipolar cell layer appeared to be well preserved even three months after the onset of symptoms (Fig.1D). This suggests that the autoantibodies reacting to TRPM1 cause dysfunction of the ON bipolar transduction pathway rather than bipolar cell death. However, further studies are needed to clarify the exact disease mechanism.

In the sera of MAR patients, several types of autoantibodies against retinal proteins have been reported, including the 22 kDa neuronal antigen GNB1, rhodopsin, S-arrestin, and aldolase-A and -C [10,16,33,34]. We initially considered that TRPM1 might be a major MAR target antigen, because TRPM1 is exclusively expressed in retinal ON bipolar cells. However, autoantibodies against TRPM1 were detected in only two out of 26 MAR patients' sera (7.7%, Fig. 4A, B). We tested whether the sera of one CAR patient and 26 MAR patients recognized human mGluR6, which is specifically expressed in ON bipolar cells, however, none of the sera exhibited a significant band in Western blot analysis (data not shown). Thus, antigens other than TRPM1 or mGluR6 may be involved in the pathogenesis of a large proportion of MAR.

Immunohistochemical analyses using the serum of the CAR patient showed labeling in the inner nuclear layer and outer plexiform layer of the adult rhesus monkey retina (Fig. 3D–G), where the bipolar cell bodies and dendrites reside, respectively. This immunostaining pattern is somewhat similar to our previous immunostaining results on the mouse retina with specific antibody against mouse TRPM1-L, which corresponds to the human TRPM1 long form [13]. Other labeling was also observed in the amacrine cells and ganglion cells. The reason for the immunoreactivity with these cells is uncertain, however, it may be due to the presence of other autoantibodies against amacrine cell and ganglion cell antigens. Lu *et al.* reported the presence of various different autoantibodies in the serum of a single PR patient [10]. If this is the case, it may explain why our CAR patient displayed severely reduced visual sensitivities in the visual field tests (Fig. 1A) unlike cCSNB patients with TRPM1 mutations[17].

It should be noted that we did not confirm whether there are any antoantibodies against TRPM1 in the sera of normal subjects by using a large number of samples. However, this possibility is thought to be low, because Shimazaki *et al.* reported that the molecular weights of the IgGs with observed anti-retinal reactivity in 92 normal sera were smaller than 148 kDa, which is smaller than the TRPM1 molecular weight of ~200 kDa, although relatively high molecular weight reactivity was not intensively investigated [35].

One limitation of the current study is that we could not obtain detailed information on the two MAR patients, MAR #8 and #23, associated with the TRPM1 autoantibody. We confirmed that these two patients had skin melanomas accompanying the visual disturbances, but could not obtain a more detailed clinical history or data on visual acuity, visual field, or ERGs because these sera were sent from different hospitals several years ago. Thus, we do not know whether these two MAR patients really had retinal ON bipolar cell dysfunction. Further prospective studies of the TRPM1 autoantibodies in large numbers of MAR patients are needed.

In conclusion, our study suggests that TRPM1 may be one of the causative antigens responsible for PR associated with ON bipolar cell dysfunction.

Note added in proof

During the course of revision process of this manuscript, Dhingra *et al.* (J. Neurosci. 31, 3962–3967, 2011) independently reported the presence of autoantibodies against TRPM1 in two MAR patients. Our study reports on autoantibodies against TRPM1 in CAR serum in addition to MAR sera.

Materials and Methods

Subjects

The Nagoya University Hospital Ethics Review Board approved this study (approval ID 1131). Of the PR patients that were examined in the Nagoya University Hospital, one PR patient with lung cancer and ON bipolar cell dysfunction was studied in detail. The examinations included routine ophthalmological and electrophysiological tests. In addition, immunohistochemical and Western blot analyses were performed using the serum of this patient. The procedures used conformed to the tenets of the Declaration of Helsinki of the World Medical Association. A written informed consent was obtained from the patient after he was provided with sufficient information on the procedures to be used.

We also obtained sera of 26 patients with MAR from two hospitals in Japan (Chiba University Hospital and Iwate Medical University Hospital) and Ocular Immunology Laboratory in the USA (Casey Eye Institute) for Western blot analysis.

Ophthalmologic examinations

The ophthalmologic examination included best-corrected visual acuity, biomicroscopy, ophthalmoscopy, fundus photography, fluorescein angiography, static perimetry, and spectral-domain optical coherence tomography (SD-OCT). Static visual fields were obtained with the Humphrey 30-2 program (Carl Zeiss, Dublin, USA), and the results are shown in gray scale. SD-OCT was performed with a 9-mm horizontal scan through the midline with 50 averages (Spectralis HRA+OCT; Heidelberg Engineering, Vista, CA).

Electroretinograms (ERG)

Full-field ERGs were elicited with a Ganzfeld dome and recorded with a Burian-Allen bipolar contact lens electrode. The ground electrode was attached to the ipsilateral ear.

After 30 minutes of dark-adaptation, a rod response was elicited with a blue light at an intensity of 5.2×10^{-3} cd-s/m^2. A cone-rod mixed maximum response was elicited by a white flash at an intensity of 44.2 cd-s/m^2. A cone response and a 30 Hz flicker response were elicited by a white stimulus of 4 cd-s/m^2 and 0.9 cd-s/m^2, respectively, on a blue background of 30 cd/m^2. Full-field cone ERGs were also elicited by long-duration flashes of 100 ms using a densely packed array of white LEDs. The array was positioned at the top of the Ganzfeld dome and covered by a diffuser. The stimulus intensity and background illumination measured in the dome was 200 cd/m^2 and 30 cd/m^2, respectively. Responses were amplified by 10K and the band pass was set to 0.3 to 1000 Hz. The data were digitized at 4.3 kHz, and 5 to 20 responses were averaged (Neuropack, Nihonkohden, Tokyo, Japan).

Immunohistochemistry

For immunohistochemistry, patient and normal sera (300 µl) were purified using the Melon Gel IgG purification kit according to the manufacturer's protocol (Pierce Biotechnology, Rockford, IL) to remove IgM, and purified sera were concentrated by Amicon Ultra 100 (Millipore, MA). The rhesus monkey eye cup was fixed with 4% paraformaldehyde in PBS for 30 min at 4°C. The samples were cryoprotected with 30% sucrose in PBS and embedded in OCT compound (Sakura Finetechnical, Tokyo, Japan). These tissues were sliced with a Microm HM 560 cryostat microtome (Microm Laborgeräte GmbH, Walldorf, Germany) into 14 µm. Sections were washed twice in PBS for 5 min, permeabilized with 0.1% Triton-X100/PBS, then washed with PBS 3 times for 5 min, and incubated with PBS containing 4% donkey serum for 1 hr to block samples. For the immunoreaction, the samples were incubated with a purified normal or CAR serum (1:300) diluted in blocking buffer at 4°C overnight. After PBS-washing, these samples were incubated with a DyLight-488 conjugated donkey anti-human IgG (H+L) (1:400) as a secondary antibody (Jackson Immunoresearch Laboratories) at room temperature for 1 hr and washed with PBS.

Transfection and Western blot analyses

HEK293T cells were cultured in D-MEM containing 10% fetal bovine serum (FBS; Nissui, Tokyo, Japan). These cells were grown under 5% carbon dioxide at 37°C. The calcium phosphate method was used to transfect the cells. Transfected cells were incubated at 37°C for 48 hrs, and then harvested for further analysis. The proteins extracted from the cells were separated by SDS–PAGE on a 7.5% precast gel (ATTO, Tokyo, Japan), and then transferred to a polyvinylidene difluoride membrane using the Invitrogen iBlot system (Invitrogen, Carlsbad, CA, USA). The membrane was incubated with primary antibodies, mouse anti-Flag (1:1,000; Sigma, St Louis, MO), sera from patients (1:100), normal human serum (1:100), or mouse anti-β-actin (1:5,000; Sigma). The membrane was then incubated with a horseradish peroxidase-conjugated goat anti-mouse IgG (1:10,000; Zymed Laboratories, San Francisco, CA) or donkey anti-human IgG (1:10,000; Jackson Immuno Research Laboratories, West Grove, PA) as secondary antibodies. The bands were developed using Chemi-Lumi One L (Nacalai Tesque, Kyoto, Japan).

Acknowledgments

We thank Richaed G. Weleber, Yozo Miyake, and Duco I. Hamasaki for helpful discussions of this study, Junko Hanaya for collecting the serum of our patients, and Mikiko Kadowaki, Aiko Ishimaru, Kaori Sone, and Shawna Kennedy for technical assistance.

Author Contributions

Conceived and designed the experiments: MK TF. Performed the experiments: MK RS SU YN NH. Analyzed the data: MK RS SU TF. Contributed reagents/materials/analysis tools: MK SU HO SY SM HT GA. Wrote the paper: MK TF. Supervised the project: MK HT TF.

References

1. Thirkill CE, FitzGerald P, Sergott RC, Roth AM, Tyler NK, et al. (1989) Cancer-associated retinopathy (CAR syndrome) with antibodies reacting with retinal, optic-nerve, and cancer cells. N Engl J Med 321: 1589–1594.
2. Chan JW (2003) Paraneoplastic retinopathies and optic neuropathies. Surv Ophthalmol 48: 12–38.
3. Heckenlively JR, Ferreyra HA (2008) Autoimmune retinopathy: A review and summary. Semin Immunopathol 30: 127–134.
4. Adamus G (2009) Autoantibody targets and their cancer relationship in the pathogenicity of paraneoplastic retinopathy. Autoimmun Rev 8 410–414.

5. Thirkill CE, Roth AM, Keltner JL (1987) Cancer-associated retinopathy. Arch Ophthalmol 105: 372–375.
6. Jacobson DM, Thirkill CE, Tipping SJ (1990) A clinical triad to diagnose paraneoplastic retinopathy. Ann Neurol 28: 162–167.
7. Milam AH, Saari JC, Jacobson SG, Lubinski WP, Feun LG, et al. (1993) Autoantibodies against retinal bipolar cells in cutaneous melanoma-associated retinopathy. Invest Ophthalmol Vis Sci 34: 91–100.
8. Alexander KR, Fishman GA, Peachey NS, Marchese AL, Tso MOM (1992) "On" response defect in paraneoplastic night blindness with cutaneous malignant melanoma. Invest Ophthalmol Vis Sci 33: 477–483.
9. Lei B, Bush RA, Milam AH, Sieving PA (2000) Human melanoma-associated retinopathy (MAR) antibodies alter the retinal ON-response of the monkey ERG in vivo. Invest Ophthalmol Vis Sci 41: 262–266.
10. Lu Y, Jia L, He S, Hurley MC, Leys MJ, et al. (2009) Melanoma-associated retinopathy: a paraneoplastic autoimmune complication. Arch Ophthalmol 127: 1572–1580.
11. Jacobson DM, Adamus G (2001) Retinal anti-bipolar cell antibodies in a patient with paraneoplastic retinopathy and colon carcinoma. Am J Ophthalmol 131: 806–808.
12. Goetgebuer G, Kestelyn-Stevens AM, De Laey JJ, Kestelyn P, Leroy BP (2008) Cancer-associated retinopathy (CAR) with electronegative ERG: a case report. Doc Ophthalmol 116: 49–55.
13. Koike C, Obara T, Uriu Y, Numata T, Sanuki R, et al. (2010) TRPM1 is a component of the retinal ON bipolar cell transduction channel in the mGluR6 cascade. Proc Natl Acad Sci U S A 107: 332–337. Epub Dec. 4, 2009.
14. Koike C, Numata T, Ueda H, Mori Y, Furukawa T (2010) TRPM1: A vertebrate TRP channel responsible for retinal ON bipolar function. Cell Calcium 48: 95–101.
15. Morgans CW, Zhang J, Jeffrey BG, Nelson SM, Burke NS, et al. (2009) TRPM1 is required for the depolarizing light response in retinal ON-bipolar cells. Proc Natl Acad Sci U S A 106: 19174–19178.
16. Hartmann TB, Bazhin AV, Schadendorf D, Eichmüller SB (2005) SEREX identification of new tumor antigens linked to melanoma-associated retinopathy. Int J Cancer 114: 88–93.
17. Nakamura M, Sanuki R, Yasuma TR, Onishi A, Nishiguchi KM, et al. (2010) TRPM1 mutations are associated with the complete form of congenital stationary night blindness. Mol Vis 16: 425–437.
18. Li Z, Sergouniotis PI, Michaelides M, Mackay DS, Wright GA, et al. (2009) Recessive mutations of the gene TRPM1 abrogate ON bipolar cell function and cause complete congenital stationary night blindness in humans. Am J Hum Genet 85: 711–719.
19. van Genderen MM, Bijveld MM, Claassen YB, Florijn RJ, Pearring JN, et al. (2009) Mutations in TRPM1 are a common cause of complete congenital stationary night blindness. Am J Hum Genet 85: 730–736.
20. Audo I, Kohl S, Leroy BP, Munier FL, Guillonneau X, et al. (2009) TRPM1 is mutated in patients with autosomal-recessive complete congenital stationary night blindness. Am J Hum Genet 85: 720–729.
21. Miyake Y, Yagasaki K, Horiguchi M, Kawase Y, Kanda T (1986) Congenital stationary night blindness with negative electroretinogram: A new classification. Arch Ophthalmol 104: 1013–1020.
22. Bech-Hansen NT, Naylor MJ, Maybaum TA, Sparkes RL, Koop B, et al. (2000) Mutations in NYX, encoding the leucine-rich proteoglycan nyctalopin, cause X-linked complete congenital stationary night blindness. Nat Genet 26: 319–23.
23. Pusch CM, Zeitz C, Brandau O, Pesch K, Achatz H, et al. (2000) The complete form of X-linked congenital stationary night blindness is caused by mutations in a gene encoding a leucine-rich repeat protein. Nat Genet 26: 324–327.
24. Dryja TP, McGee TL, Berson EL, Fishman GA, Sandberg MA, et al. (2005) Night blindness and abnormal cone electroretinogram ON responses in patients with mutations in the GRM6 gene encoding mGluR6. Proc Natl Acad Sci USA 102: 4884–4889.
25. Miyake Y, Yagasaki K, Horiguchi M, Kawase Y (1987) On- and off-responses in photopic electroretinogram in complete and incomplete types of congenital stationary night blindness. Jpn J Ophthalmol 31: 81–87.
26. Houchin K, Purple RL, Wirtschafter JD (1991) X-linked congenital stationary night blindness and depolarizing bipolar system dysfunction. [ARVO abstract] Invest Ophthalml Vis Sci 32: S1229.
27. Young RSL (1991) Low-frequency component of the photopic ERG in patients with X-linked congental stationary night blindness. Clin Vis Sci 6: 309–315.
28. Khan NW, Kondo M, Hiriyanna KT, Jamison JA, Bush RA, et al. (2005) Primate retinal signaling pathways: Suppressing ON-pathway activity in monkey with glutamate analogues mimics human CSNB1-NYX genetic night blindness. J Neurophysiol 93: 481–492.
29. Polans AS, Witkowska D, Haley TL, Amundson D, Baizer L, et al. (1995) Recoverin, a photoreceptor-specific calcium-binding protein, is expressed by the tumor of a patient with cancer-associated retinopathy. Proc Natl Acad Sci U S A 92: 9176–9180.
30. Matsubara S, Yamaji Y, Sato M, Fujita J, Takahara J (1996) Expression of a photoreceptor protein, recoverin, as a cancer-associated retinopathy autoantigen in human lung cancer cell lines. Br J Cancer 74: 1419–1422.
31. Ohguro H, Odagiri H, Miyagawa Y, Ohguro I, Sasaki M, et al. (2004) Clinicopathological features of gastric cancer cases and aberrantly expressed recoverin. Tohoku J Exp Med 202: 213–219.
32 Bazhin AV, Schadendorf D, Willner N, De Smet C, Heinzelmann A, et al. (2007) Photoreceptor proteins as cancer-retina antigens. Int J Cancer 120: 1268–76.
33. Keltner JL, Thirkill CE (1999) The 22-kDa antigen in optic nerve and retinal diseases. J Neuroophthalmol 19: 71–83.
34. Potter MJ, Adamus G, Szabo SM, Lee R, Mohaseb K, et al. (2002) Autoantibodies to transducin in a patient with melanoma-associated retinopathy Am J Ophthalmol 134: 128–30.
35. Shimazaki K, Jirawuthiworavong GV, Heckenlively JR, Gordon LK (2008) Frequency of anti-retinal antibodies in normal human serum. J Neuro-Ophthalmol 28: 5–11.

Doc Ophthalmol (2011) 123:127–133
DOI 10.1007/s10633-011-9286-x

CASE REPORT

Oguchi disease masked by retinitis pigmentosa

Hiroko Sonoyama · Kei Shinoda · Chie Ishigami · Yumi Tada · Hidenao Ideta · Ryuichi Ideta · Masayo Takahashi · Yozo Miyake

Received: 11 June 2011 / Accepted: 25 August 2011 / Published online: 16 September 2011

Abstract The purpose of this study was to report a patient with Oguchi disease whose ophthalmological characteristics were masked by retinitis pigmentosa (RP). The method used in this study was case report. A 53-year-old man had a progressive decrease in his visual acuity and was diagnosed with RP because of night blindness, fundoscopic findings, ring scotoma, and extinguished single-flash electroretinograms (ERGs). However, a faint golden-yellowish reflex of the retina prompted us to make a more detailed examination of the fundus after a long period of dark adaptation, ERGs, and genetic analysis. Examinations showed the Mizuo-Nakamura phenomenon, relative intact photopic ERGs, and a *SAG* mutation, and the patient was diagnosed with RP associated with Oguchi disease. When RP accompanies Oguchi disease, the clinical characteristics of Oguchi disease might be masked. In such a situation, the correct diagnosis is difficult. However, careful analysis of clinical findings will suggest Oguchi disease, which can be confirmed by molecular genetics.

Keywords Oguchi disease · Mizuo-Nakamura phenomenon · SAG1 gene · Retinitis pigmentosa

H. Sonoyama · H. Ideta · R. Ideta · Y. Miyake
Ideta Eye Hospital, Kumamoto, Japan

K. Shinoda (✉)
Department of Ophthalmology, Teikyo University School of Medicine, 2-11-1 Kaga, Itabashi-ku, Tokyo 173-8605, Japan
e-mail: shinodak@med.teikyo-u.ac.jp

C. Ishigami · Y. Tada · M. Takahashi
RIKEN Center for Developmental Biology, Kobe, Japan

Y. Miyake
Aichi Medical University, Aichi, Japan

Introduction

Oguchi disease, first described [1] in 1907, is a rare autosomal recessive form of congenital stationary night blindness. It is characterized by a yellowish-gold fundus that disappears after prolonged dark adaptation, the Mizuo-Nakamura phenomenon. In general, the visual acuity, visual fields, and color vision are normal in patients with Oguchi disease [2]. The full-field rod electroretinograms (ERGs) after 30 min of dark adaptation are non-recordable but the cone and 30-Hz flicker ERGs are essentially normal. The a-wave of the mixed rod–cone ERGs elicited by a bright flash is significantly reduced, the b-wave is non-detectable, and the oscillatory potentials are well preserved [2, 3].

There are two genes that cause Oguchi disease: the G protein-coupled receptor kinase 1 gene (*GRK1*; MIM, 180381) and the *S* antigen gene (*SAG*; MIM, 181031) [4, 5]. There is evidence that Oguchi disease and retinitis pigmentosa (RP) can coexist in the same family or even in the same individual [6–8]. Only little information is available on genetically confirmed

cases of Oguchi disease with concomitant RP-like fundus appearance [9–13]. We report a case of genetically confirmed Oguchi disease that had typical characteristics of RP.

Case report

A 53-year-old man who had night blindness since his childhood was diagnosed with RP in an eye clinic in his neighborhood. He was referred to the Ideta Eye Clinic for further examination in 2008. His visual acuity had been 1.5 OU without correction but decreased in his thirty's. He had no family history, and his parents were not consanguineous. On examination, his best-corrected decimal visual acuity was 0.4 OD and 0.2 OS. Ophthalmoscopy showed diffuse changes in the retinal pigment epithelium (RPE), depigmented spots along the arcade vessels that extended to the mid-peripheral region, and bone corpuscle-like deposits (Fig. 1). Neither optic disk pallor nor atrophy was found, and a narrowing of retinal vessels was minimal. Cystoid macular edema (CME) was present, and a well-demarcated golden-yellowish reflex with Mizuo-Nakamura phenomenon was observed in the inferior peripheral area (Fig. 1). Fluorescein angiography (FA) showed window defects and granular hyperfluorescence corresponding to the RPE changes and pooling of the dye in the CME (Fig. 1). No special FA changes were observed in the area of golden-yellowish reflex. A ring scotoma and decreased sensitivity in the central area were detected

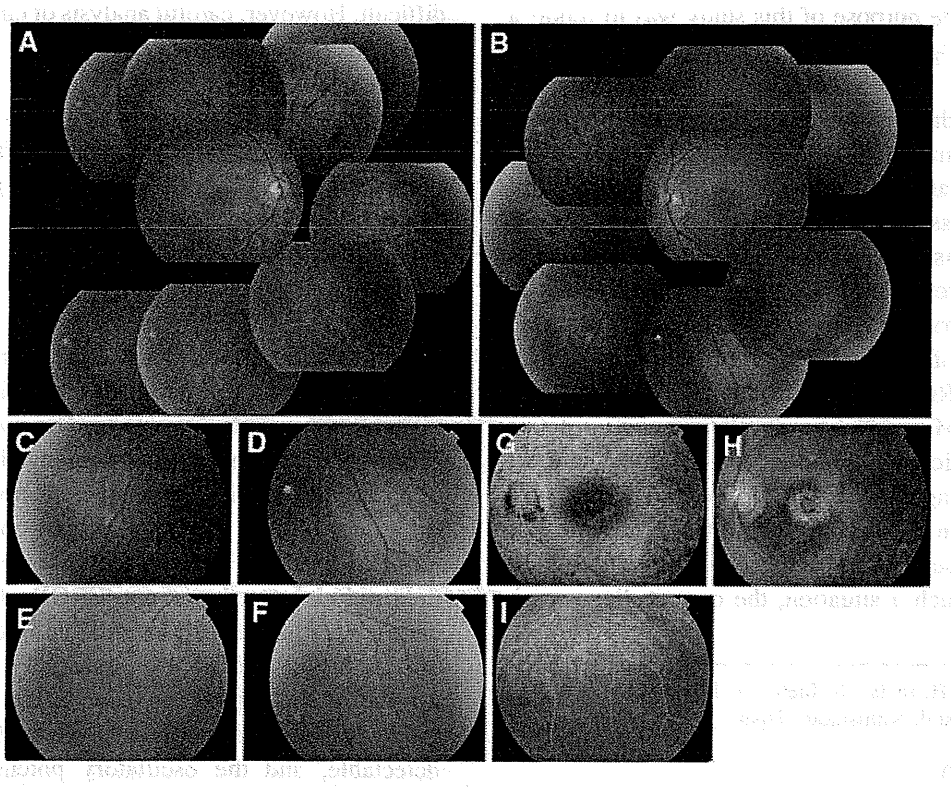

Fig. 1 Fundus photographs and fluorescein angiograms of a patient with Oguchi disease. **a**, **b** Fundus photographs of the *right* (**a**) and *left* (**b**) eyes showing diffuse changes in the retinal pigment epithelium, depigmented spots along the arcade vessels extending to the mid-peripheral region, and bone corpuscle-like deposits. Neither optic disk pallor nor atrophy can be seen, and the narrowing of retinal vessels was minimal. **c**, **d** The inferior peripheral fundus photographs of the *left* eye showing well-demarcated *golden-yellowish* reflex. **e**, **f** The inferior peripheral fundus photographs of the *left* eye corresponding to **c** and **d**, respectively, after 3 h of dark adaptation. The *golden-yellowish* reflex disappeared, suggesting Mizuo-Nakamura phenomenon. **g–i** Fluorescein angiograms of the *left* eye. Fundus photographs of the posterior pole at early phase (**g**) and late phase (**h**) showing window defect and granular hyperfluorescence corresponding to the changes in the retinal pigment epithelium and pooling of the dye at the cystoid macular edema. No special findings can be seen at the area of *golden-yellowish* reflex (**i**)

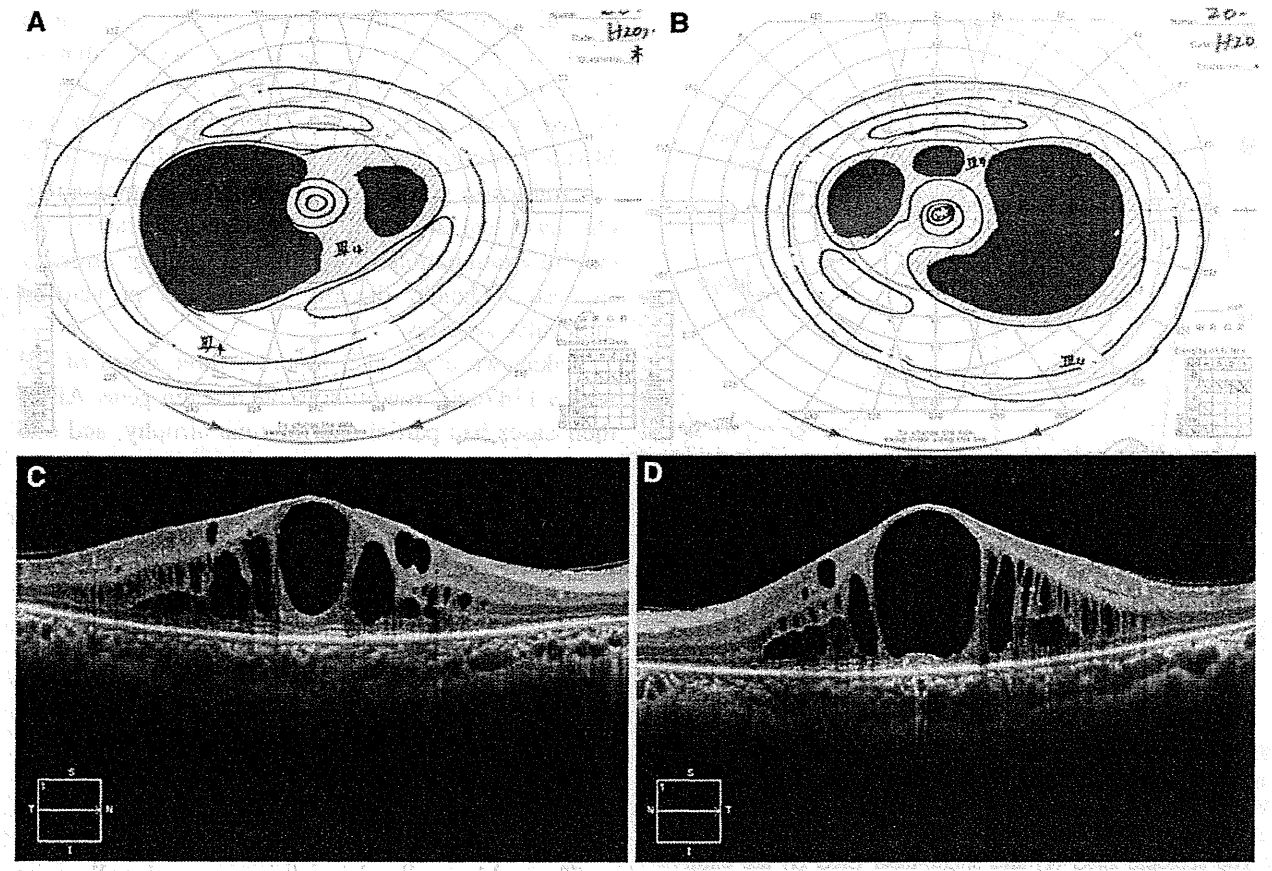

Fig. 2 Goldmann visual fields and optical coherence tomographic (OCT) images of a patient with Oguchi disease. **a**, **b** Visual fields of the *left* (**a**) and *right* (**b**) eyes showing ring scotomas and decreased sensitivity in the central area. **c**, **d** OCT (Cirrus HD-OCT) images of the *right* (**c**) and *left* (**d**) eyes showing severe cystoid macular edema and the border of the photoreceptor inner and outer segments (IS/OS *line*) were partially indiscernible or discontinued. These findings were more marked in the *left* eye

by Goldmann perimetry (Fig. 2). Optical coherence tomography (OCT Cirrus HD-OCT) showed severe CME, and the border of the photoreceptor inner and outer segments (IS/OS line) was not clear and where it was seen it was discontinuous. The changes were more apparent in the left eye (Fig. 2).

Full-field ERGs were recorded according to the International Society for Clinical Electrophysiology of Vision (ISCEV) protocol, and the scotopic (rod) ERGs and single-flash mixed rod–cone ERGs after 30 min of dark adaptation were abolished. The amplitudes of the photopic cone responses were approximately 50% of that of normal subjects, while the 30-Hz flicker ERG was relatively well preserved (Fig. 3). The mixed rod–cone ERG did not change even after 3 and 6 h of dark adaptation. The multifocal ERGs were diffusely reduced in the right eye and almost extinguished throughout the recording area in the left eye.

A diagnosis of RP seemed to be correct, but we detected some subtle signs which suggested Oguchi disease and we performed further genetic studies.

Molecular genetic studies

The research protocol was approved by the Ethics Review Board of Ideta Eye Clinic. The protocol adhered to the tenets of the Declaration of Helsinki, and an informed consent was obtained from the patient.

The coding regions of *SAG/arrestin* and *GRK1/RHOK* were amplified by polymerase chain reaction and were analyzed using direct sequencing in both directions. The coding regions of 34 genes responsible for autosomal dominant RP were also analyzed. A homozygous mutation of c.926delA (N309TfX320)

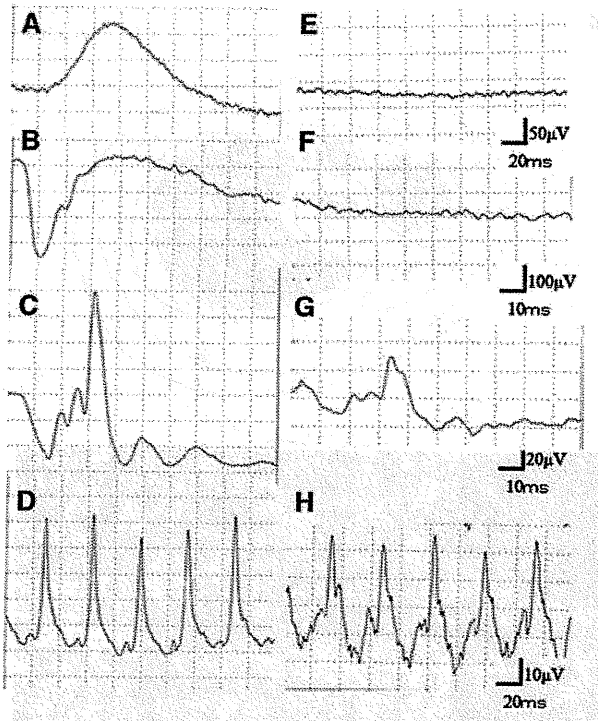

Fig. 3 Full-field electroretinograms (ERGs) recorded according to the International Society for Clinical Electrophysiology of Vision (ISCEV) protocol from a normal subject (*left column* **a–d**) and our patient with Oguchi disease (*right column* **e–f**). **e, f** The scotopic ERG (**e**) and single-flash ERG (**f**) are extinguished. **g** The cone (**g**) responses are reduced by approximately 50% of that of normal subject (**c**). **h** The 30-Hz flicker ERG is relatively preserved

was identified in exon 11 of the *SAG* gene. No other mutations were found in any other coding regions.

Discussion

Our case was initially diagnosed as typical RP from the progressive, diffuse RPE atrophy associated with bone corpuscle-like deposits, bilateral CME, ring scotoma, extinguished mixed rod–cone ERG, and no improvement in ERG after prolonged dark adaptation. However, faint localized areas of golden-yellowish reflex of the fundus attracted our attention. Further examination revealed several signs characteristic of Oguchi disease: viz., night blindness since his childhood, Mizuo-Nakamura phenomenon, slight or no optic disk atrophy, slight narrowing of the retinal vessel, and recordable cone ERGs, which were masked by typical features of RP. A Pubmed search extracted only 5 cases of genetically confirmed Oguchi disease with RP-like fundus appearance (Table 1) [9–13]. All of these cases except that of Nakazawa [12] were easily diagnosed as Oguchi disease from the golden-colored fundus with the Mizuo-Nakamura phenomenon, and all had only sectoral chorioretinal atrophy and/or pigmentation. Our case had a typical RP fundus appearance, but careful examination of the clinical findings strongly suggested Oguchi disease, which was proven by molecular genetics.

Nakazawa et al. [12] reported three cases of RP with a 1147delA mutation in the arrestin gene. All of their cases had partial chorioretinal atrophy, and one of them had pigmentary retinal degeneration that extended from the macular area to the mid-peripheral retina. In addition, this patient had an abnormal golden-yellow fundus reflex in the peripheral area that showed the Mizuo-Nakamura phenomenon.

They concluded that the arrestin 1147delA, which has been known as a frequent cause of Oguchi disease, also may be related to the pathogenesis of autosomal recessive RP. Our case clearly showed that the same individual can have the typical findings of RP and Oguchi disease with the mutation. Thus, our findings strongly support their conclusion.

The golden-yellowish reflex is occasionally seen in young normal individuals especially in the peripheral area. Our case suggests that such retinal reflexes may be a subtle sign of Oguchi disease, and checking for the presence of the Mizuo-Nakamura phenomenon might be of great help in the diagnosis. The pathology or mechanism of the Mizuo-Nakamura phenomenon has not been fully determined. No golden-yellowish reflex was observed at the area with RPE degeneration in our case. This suggests that such reflex and Mizuo-Nakamura phenomenon may be related to RPE change. Further careful attention on the retinal area of golden-yellowish reflex will be important.

CME is known to be associated with RP, but no case of Oguchi disease with CME has been reported. Its presence in our case also hampered our diagnosis of Oguchi disease.

Our ERG findings showed that the b-wave of the photopic cone ERG was present but was almost extinguished in the mixed ERGs. One explanation for this is that the b-wave of the mixed ERGs was greatly reduced by the photopic hill phenomenon i.e., the amplitude of the b-wave increases with increasing

Table 1 Previous reports on coexistent Oguchi disease and retinitis pigmentosa in a same family or same individual associated with *SAG* mutation

No.	Author	Year	Ref.	Mutation	Gender (age)	
					Oguchi disease	RP
Same family						
F1	Yoshii et al.	1998	[17]	N309 (1-bp del) homo	M (45), F (42)	M (52)
F2	Nakazawa et al.	1998	[12]	N309 (1-bp del) homo	F (55)	M (58)
F3	Maw et al.	1998	[9]	R193X homo	M (28)*	M (18)*

						Fundus findings	Mizuo-Nakamura phenomenon	Visual field defect	Bright flash ERG	Scotopic rod ERG	Photopic cone ERG
Same individual											
C1	Nakamachi et al.	1994	[13]	N309 (1-bp del) homo	M (54)	Typical Oguchi disease with sectoral RP	(+)	(+)	Mildly diminished a-wave and extinguished b-wave	Extinguished b-wave	n.m.
C2	Nakazawa et al.	1997	[10]	N309 (1-bp del) homo	F (58)	Typical Oguchi disease with sectoral RP	(+)	(+)	Diminished a-wave and extinguished b-wave	Extinguished	well preserved
C3	Nakazawa et al.	1998	[12]	N309 (1-bp del) homo	M (35)	Typical RP with sectral Oguchi disease	(+)	n.m.	Severely diminished a-wave and extinguished b-wave	n.m.	n.m.
C4	Maw et al.	1998	[9]	R193X homo	M (18)	Typical Oguchi disease OD and typical RP OS	n.m.	n.m.	(OD) white flash elicited a negative wave and the response to blue flash was extinguished	(OS) extinguished	(OS) extinguished
C5	Hayashi et al.	2011	[11]	N309 (1-bp del) homo	M (63)	Typical Oguchi disease with Sectoral RP	(+)	(+)	Diminished a-wave and extinguished b-wave	Extinguished	Diminished
C6	The current case			N309 (1-bp del) homo	M (53)	Typical RP with sectral Oguchi disease	(+)	(+)	Almost extinguished	Extinguished	Diminished

F2 and C3, F3 and C4 are same reports

M male, *F* female, *RP* retinitis pigmentosa, *n.m.* not mentioned

* They are two of three siblings, and the elder showed typical Oguchi OU and the younger showed Oguchi OD and RP OS

stimulus intensities at lower intensities, reaches a plateau, and then decreases at higher stimulus intensities [14]. Because rod responses are extinguished in Oguchi disease, the mixed ERGs might be affected by this phenomenon. In our case, the cone responses were also reduced due to progression of the disease process. Therefore, the b-wave of the mixed ERGs appeared to be almost extinguished. These ERG findings have not been reported even in cases with a coexistence of Oguchi disease and RP (Table 1). Therefore, further examinations in such cases will be helpful to clarify the reason of the discrepancy between the b-waves of the photopic ERGs and the mixed ERGs.

Mutations in the *SAG* gene are known to cause Oguchi disease in the Japanese [10, 11, 15, 16]. It has also been reported that *SAG* may cause RP [16–18]. In fact, several reports suggest that Oguchi disease and RP can coexist in the same family or even in the same individual [9–13, 17] (Table 1). Four mutations in the arrestin gene, R175X, R193X, N309T, and R292X, have been reported [9–12], and their phenotypes varied from typical Oguchi disease to that of RP. These non-sense or frameshift mutations with premature termination of protein translation may cause different protein products leading to dysfunction in the visual cycle, which results in the phenotypic variations. But it is still not known why the same mutation region of arrestin has such phenotypic variations [18].

In addition to the phenotypic heterogeneity of Oguchi disease, Oguchi patients can develop RP at an advanced stage [19]. The first case of Oguchi disease was reported to develop typical RP later in life [20]. In addition, atypical cases of Oguchi disease with this mutation had progressive visual field defects, reduced cone ERGs, and regional chorioretinal atrophy [9–11, 13]. In such cases, fundoscopic and electroretinographic features of Oguchi disease would be masked and careful attention on the very slight alterations is important. It is also necessary to follow patients with Oguchi disease carefully for a longer period keeping in mind the possibility of RP development.

Acknowledgments No author has a financial or proprietary interest in any material or method mentioned. Support of this study was provided by Research Grants from the Ministry of Health, Labor, and Welfare, Japan.

Conflict of interest None.

References

1. Oguchi C (1907) On a type of night-blindness. Acta Soc Ophthalmol Jpn 11:123–134 (Japanese)
2. Miyake Y (2006) Oguchi's disease. In: Miyake Y (ed) Electrodiagnosis of retinal diseases. Springer, Tokyo, pp 119–122
3. Miyake Y, Horiguchi M, Suzuki S, Kondo M, Tanikawa A (1996) Electrophysiological findings in patients with Oguchi's disease. Jpn J Ophthalmol 40:511–519
4. Fuchs S, Nakazawa M, Maw M, Tamai M, Oguchi Y, Gal A (1995) A homozygous 1-base pair deletion in the arrestin gene is a frequent cause of Oguchi disease in Japanese. Nat Genet 10:360–362
5. Yamamoto S, Sippel KC, Berson EL, Dryja TP (1997) Defects in the rhodopsin kinase gene in the Oguchi form of stationary night blindness. Nat Genet 15:175–178
6. Tanaka K (1942) A case of Oguchi's disease with retinitis pigmentosa. Jpn Rev Clin Ophthalmol 37:1237 (Japanese)
7. Shimizu S (1942) A family with Oguchi's disease and with retinitis pigmentosa accompanied with glaucoma. Jpn Rev Clin Ophthalmol 40:218–219 (Japanese)
8. Yamanaka M (1969) Histologic study of Oguchi's disease. Its relationship to pigmentary degeneration of the retina. Am J Ophthalmol 68:19–26
9. Maw M, Kumaramanickave G, Kar B, Kar B, John S, Bridges R, Denton M (1998) Two Indian siblings with Oguchi disease are homozygous for an arrestin mutation encoding premature termination. Hum Mutat (Suppl 1): S317–S319
10. Nakazawa M, Wada Y, Fuchs S, Gal A, Tamai M (1997) Oguchi disease: phenotypic characteristics of patients with the frequent 1147delA mutation in the arrestin gene. Retina 17:17–22
11. Hayashi T, Tsuzuranuki S, Kozaki K, Urashima M, Tsuneoka H (2011) Macular dysfunction in Oguchi disease with the frequent mutation 1147delA in the SAG gene. Ophthalmic Res 46:175–180
12. Nakazawa M, Wada Y, Tamai M (1998) Arrestin gene mutations in autosomal recessive retinitis pigmentosa. Arch Ophthalmol 116:498–501
13. Nakamachi Y, Nakamura M, Fujii S, Yamamoto M, Okubo K (1998) Oguchi disease with sectoral retinitis pigmentosa haboring adenine deletion at position 1147 in the arrestin gene. Am J Ophthalmol 125:249–251
14. Wali L, Leguire LE (1992) The photopic hill: a new phenomenon of the light adapted electroretinogram. Doc Ophthalmol 80:335–342
15. Nakamura M, Yamamoto S, Okada M, Ito Y, Miyake Y (2004) Novel mutations in the arrestin gene and associated clinical features in Japanese patients with Oguchi's disease. Ophthalmology 111:1410–1414
16. Saga M, Mashima Y, Kudoh J, Oguchi Y, Shimizu N (2004) Gene analysis and evaluation of the single founder effect in Japanese patients with Oguchi disease. Jpn J Ophthalmol 48:350–352
17. Yoshii M, Murakami A, Akeo K, Nakamura A, Shimoyama M, Ikeda Y, Kikuchi Y, Okisaka S, Yanashima K, Oguchi Y (1998) Visual function and gene analysis in family with Oguchi disease. Ophthalmic Res 30:394–401

18. Gurevich VV, Gurevich EV (2006) The structural basis of arrestin-mediated regulation of G-protein-coupled receptors. Pharmacol Ther 110:465–502
19. Isashiki Y, Ohba N, Kimura K, Sonoda S, Kakiuchi T, Ozawa T (1999) Retinitis pigmentosa with visual fluctuation and arrestin gene mutation. Br J Ophthalmol 83:1197–1198
20. Majima K (1954) Report of a patient with Oguchi disease. Jpn Rev Clin Ophthalmol 48:121 (Japanese)

VITRECTOMY FOR PROLIFERATIVE RETINOPATHY IN PATIENT WITH ADVANCED DUCHENNE MUSCULAR DYSTROPHY

Keitetsu So, MD,*† Kei Shinoda, MD, PhD,† Emiko Watanabe, MD, PhD,†
Toru Mashiko, MD,* Atsushi Mizota, MD, PhD†

Purpose: Retinal vascular abnormalities are rare in patients with Duchenne muscular dystrophy. We present a patient with Duchenne muscular dystrophy who developed severe proliferative retinopathy for which vitrectomy was successfully performed in one eye.

Method: Case presentation. A 23-year-old Japanese man with Duchenne muscular dystrophy complicated by cardiac and respiratory insufficiency had reduced vision in both eyes. His best-corrected visual acuity was 0.01 in the right eye and hand movements in the left eye. Ophthalmoscopy showed vitreous hemorrhage and proliferative tissue attached to the optic disk bilaterally. Ultrasound echography showed tractional retinal detachment in the left eye.

Results: Because general anesthesia was considered to be a high risk, vitrectomy, lensectomy, neovascular membrane removal, endolaser photocoagulation, and silicone oil injection were performed under local anesthesia on the right eye. After removal of the silicone oil and intraocular lens implantation, the best-corrected visual acuity was 0.8 in the right eye. Vitrectomy was performed on the left eye, but the retina could not be attached.

Conclusion: The etiology of the proliferative retinopathy in our case is not known. Because early treatment has the potential to improve and maintain vision, we recommend periodic fundus examinations in patients with Duchenne muscular dystrophy.

RETINAL CASES & BRIEF REPORTS X:1–3, 2011

AQ : 1

*From the *Department of Ophthalmology, Teikyo University School of Medicine, University Hospital Mizonokuchi, Kawasaki, Japan; and †Department of Ophthalmology, Teikyo University School of Medicine, University Hospital Itabashi, Tokyo, Japan.*

Duchenne muscular dystrophy (DMD) is the most common form of X-linked recessive neuromuscular disorder,[1–3] with an incidence of 1 in 3,500 live-born male infants. The major clinical manifestation of DMD usually appears around 3 years to 5 years of age and is progressive. By age 12, most patients become wheelchair-dependent and develop fixed contractures and scoliosis. By age 16 to 18, patients are predisposed to serious, sometimes fatal, pulmonary infections.

Abnormal retinal neurotransmission is associated with a mutation in the dystrophin gene,[4–6] and retinal vascular abnormalities have also been reported in few cases of DMD.[7,8] We have examined a patient with DMD who developed severe proliferative retinopathy in both eyes, and retinal reattachment was achieved by vitreous surgery in one eye but was not achieved in the other eye.

Supported by the Research Grants on Sensory and Communicative Disorders from the Ministry of Health, Labor, and Welfare, Japan, and by the Ministry of Education, Culture, Sports, Science and Technology, Japan.

The authors report no financial or conflicts of interest to disclose.

Reprint requests: Kei Shinoda, MD, Department of Ophthalmology, Teikyo University School of Medicine, 2-11-1 Kaga, Itabashi-ku, Tokyo,173-8605, Japan, e-mail: shinodak@med.teikyo-u.ac.jp

Case Report

A 23-year-old Japanese man was referred to us in November 2008 for the diagnosis and treatment of decreased vision of 4 weeks duration in both eyes. The patient had DMD, which was